PHYSICAL REVIEW E **94**, 011101(R) (2016)

Elastic wave turbulence and intermittency

Sergio Chibbaro and Christophe Josserand

Sorbonne Universités, UPMC Univ Paris 06, UMR 7190, Institut Jean Le Rond d'Alembert, F-75005, Paris, France
and CNRS, UMR 7190, Institut Jean Le Rond d'Alembert, F-75005, Paris, France

(Received 11 November 2015; published 8 July 2016)

We investigate the onset of intermittency for vibrating elastic plate turbulence in the framework of the weak wave turbulence theory using a numerical approach. The spectrum of the displacement field and the structure functions of the fluctuations are computed for different forcing amplitudes. At low forcing, the spectrum predicted by the theory is observed, while the fluctuations are consistent with Gaussian statistics. When the forcing is increased, the spectrum varies at large scales, corresponding to the oscillations of nonlinear structures made of ridges delimited by *d* cones. In this regime, the fluctuations exhibit small-scale intermittency that can be fitted via a multifractal model. The analysis of the nonlinear frequency shows that the intermittency is linked to the breakdown of the weak turbulence at large scales only.

DOI: 10.1103/PhysRevE.94.011101

Introduction. Random interacting waves, often called wave turbulence [1–3], are present in different systems such as oceans [4–6], capillary or Alvèn waves [7–10], nonlinear optics [11], and elastic plates [12]. Understanding the statistical properties of such structures is crucial since intermittency and/or anomalous scalings may have important practical interest, for instance in predicting the frequency of extreme events such as rogue waves in oceans [6,13]. At variance with hydrodynamics turbulence, a linear order is present, consisting of independent dispersive waves, and a perturbative statistical approach converges asymptotically for weak nonlinearities, the so-called weak wave turbulence theory (WWT) [1–3]. WWT can be seen as a mean-field theory for the spectrum $n(\mathbf{k},t)$, which neglects fluctuations and supports nonequilibrium cascade solutions. The asymptotic closure suggests that the Fourier modes are somehow close to joint Gaussianity, even though it is not a necessary condition and the detailed statistics of the fluctuations is still debated [3]. Indeed, large discrepancies with the WWT predictions have been observed in some cases [14], motivating the theoretical analysis of possible onset of strong fluctuations and intermittency [10,15–22]. Moreover, when nonlinearities are not weak anymore, a breakdown of weak turbulence occurs, since the WWT is not formally valid, and anomalous scalings for the fluctuations are then expected. Nevertheless, turbulent spectra are usually still observed, involving the spectrum of strong nonlinear dynamical structures, leading, for example, to the so-called Phillips spectrum [23,24]. First evidences of these nontrivial behaviors have been observed for gravity waves both numerically [25] and experimentally [26–28]. However, because of the difficulties of gravity wave dynamics [27,29], a detailed understanding of the origin of this intermittent behavior is still lacking. In fact, although a potential link between the breakdown of WWT and the appearance of intermittency has been invoked, the underlying mechanisms need still to be identified.

The goal of this Rapid Communication is to investigate the occurrence of intermittency and the breakdown of WWT by analyzing numerically the vibrations of elastic plates, prototype of wave turbulence [12,30], that is also well suited for experimental investigations [31–34].

Wave turbulence in plates. Elastic vibrating plates are modeled using the dynamical version of the Föppl–von Kármán (FVK) equations [35]. These equations describe the evolution of the out-of-plane displacement $\zeta(x,y,t)$ of a plane plate of thickness h of an elastic material of density ρ, Young modulus E, and Poisson coefficient σ. It reads in a dimensionless form:

$$\frac{\partial^2 \zeta}{\partial t^2} = -\frac{1}{4}\Delta^2\zeta + \{\zeta,\chi\}, \tag{1}$$

$$\Delta^2\chi = -\tfrac{1}{2}\{\zeta,\zeta\}, \tag{2}$$

where the lengths have been rescaled by $h/\sqrt{3(1-\sigma^2)}$, the time by $h\sqrt{\rho/[3E(1-\sigma^2)]}$, and the Airy stress function $\chi(x,y,t)$ that describes the plate stresses by $Eh^2/[3(1-\sigma^2)]$. $\Delta = \partial_{xx} + \partial_{yy}$ is the usual Laplacian and the bracket $\{\cdot,\cdot\}$ is defined by $\{f,g\} \equiv f_{xx}g_{yy} + f_{yy}g_{xx} - 2f_{xy}g_{xy}$, so that Eq. (1) preserves the momentum of the center of mass, namely $\partial_{tt}\int \zeta(x,y,t)dxdy = 0$. The first term on the right-hand side of (1) represents the bending while the second one $\{\zeta,\chi\}$, a cubic nonlinearity, represents the stretching. The second equation (2) relates the Airy stress function to the Gaussian curvature of the plate $\{\zeta,\zeta\}$. Linear elastic waves obey a quadratic dispersive relation $\omega_{\mathbf{k}} = k^2/2$ ($\mathbf{k}$ the wave number and $\omega_{\mathbf{k}}$ the wave frequency), so that the WWT formalism can be applied [12]. WWT consists then of a small frequency correction quantifying the (weak) nonlinear interactions:

$$\omega_{\boldsymbol{k}}^{(1)} = \frac{\pi}{2}\left[\int_0^k \frac{\omega_q q^2}{k^2}\langle|\zeta_{\boldsymbol{q}}|^2\rangle\, q dq + \int_k^\infty \frac{\omega_q k^2}{q^2}\langle|\zeta_{\boldsymbol{q}}|^2\rangle\, q dq\right], \tag{3}$$

where $\zeta_{\boldsymbol{k}} = \frac{1}{2\pi}\int \zeta(\boldsymbol{x},t)e^{i\boldsymbol{k}\cdot\boldsymbol{x}}d^2\boldsymbol{x}$ is the Fourier transform of the displacement field ζ and the brackets $\langle\cdot\rangle$ indicate statistical average. The next order of the WWT is a kinetic equation for the spectrum of the displacement $\langle|\zeta_{\boldsymbol{k}}|^2\rangle$ involving four-wave nonlinear interactions that exhibits two types of stationary solutions. In addition to the Rayleigh-Jeans *equilibrium* distribution, which reads $\langle|\zeta_{\boldsymbol{k}}|^2\rangle = \frac{T}{\omega_k}$, where T plays the role of a temperature, WWT predicts a constant flux of energy from the large- to the small-scale solution, the Kolmogorov-Zakharov

(KZ) spectrum:

$$\langle|\zeta_{\boldsymbol{k}}|^2\rangle^{KZ} = CP^{1/3}\frac{\ln^{1/3}(k_*/k)}{k^4}. \tag{4}$$

The logarithm correction comes from the degeneracy of the Rayleigh-Jean solutions, similarly to the WWT for the nonlinear Schrödinger equation in two dimensions (2D) [36,37]. P is the energy flux density involved in the energy cascade, k_* is a critical wave number, and C is a pure number.

For the present study, the FVK equations (1) and (2) are solved numerically using a pseusospectral method on a square plate with periodic boundary conditions. The linear wave dynamics is solved exactly in the Fourier space while the nonlinear terms are evaluated in the real space using fast Fourier transform [12]. Dissipation at small scales and forcing at large ones are added in Eq. (1) to simulate a turbulent process. Realistic dissipation in plates is in fact present at all scales, affecting the spectra of vibrating plates [34,38,39]. In order to avoid this problem that is not related to the present issue, we have chosen to model the dissipation using a classical diffusion process $D(\mathbf{x},\mathbf{t}) = \gamma\Delta\dot{\zeta}$, where γ represents the relevant viscosity and $\dot{\zeta}$ is the vertical velocity. It presents the advantages of being mostly relevant at small scales, in agreement with the WWT, and of remaining reasonably close to the real dissipation [34,41]. The forcing is added as a white random force at large scales, whose amplitude in Fourier space follows $V\Theta(k_0 - k)$, where $\Theta(\cdot)$ is the Heavyside function. Here, the amplitude V is varied over a large range of values with a constant characteristic wave length $k_0 = 0.05$. The simulations start with a plate at rest. Then, after a transient, a statistically stationary regime is reached, where the field and the energy are fluctuating around mean values. The amplitude V is directly related to the power injected in the system ϵ that corresponds, in this stationary regime, to the dissipation, following $\epsilon \propto V^2$.

Numerics and spectra. In Fig. 1, we show the numerical representation of the plate deflection together with the corresponding displacement spectrum, for different forcing. First, it should be emphasized that for all the spectra computed here, no anisotropy of the fields have been observed, as already noticed in experiments [40]. Two different groups of spectra are identified, separating low from high forcing regimes: For the four smallest forcing (corresponding to $V \leqslant 10^{-5}$), the k^{-4} slope is observed over an inertial range separating the forcing from the damping scales, in line with theoretical predictions. For the larger forcing ($V \geqslant 5 \times 10^{-5}$) the k^{-4} slope is still present at large wave numbers, whereas a steeper spectrum consistent with $|\zeta_{\boldsymbol{k}}|^2 \sim k^{-6}$ appears at low wave numbers, as recently highlighted experimentally and numerically [33]. There, most of the energy is concentrated in coherent deformations, which have been identified to be dynamical ridges limited by d cones. More precisely, since ridges correspond to lines separating planar domain, they can be described by the relation $\partial_x\zeta \sim \Theta(x - x_0)$, where Θ is the Heavyside function. Such displacement fields exhibit a $1/k^4$ spectrum similar to the KZ one but the logarithm correction. On the other hand, one should notice that such ridges exhibit d cones at their edges whose spectra scale like $1/k^6$: Indeed, close to its center a d cone can be described in polar coordinates following $\zeta(\mathbf{x}) \sim rf(\theta)$, where

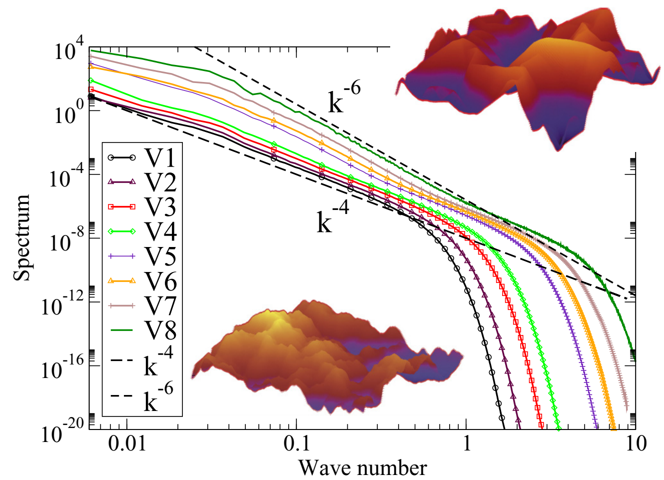

FIG. 1. Wave spectrum $\langle|\zeta_k|^2\rangle$ for the different forcings studied. We have used 8 forcing amplitudes spanning two orders of magnitude (the smallest is $V1 = 10^{-6}$ and the strongest $V8 = 5 \times 10^{-4}$, corresponding to energy flux ranging from $\epsilon = 4.45 \times 10^{-10}$ to $\epsilon = 10^{-4}$, following $\epsilon \propto V^2$). The curves correspond to increasing forcing from the bottom to the top, with $V2 = 2 \times 10^{-6}$, $V3 = 5 \times 10^{-6}$, $V4 = 10^{-5}$, $V5 = 5 \times 10^{-5}$, $V6 = 10^{-4}$, and $V7 = 2 \times 10^{-4}$. The dashed lines represent the two limit curves $|\zeta_k|^2 \sim k^{-4}$ for the theoretical Kolmogorov-Zakharov (KZ) spectrum (up to the logarithmic correction) and k^{-6} that describes the ridge turbulence. In all the simulations, the plate is a 1024×1024 square and in order to correctly describe the high forcing amplitudes, we have varied accordingly the mesh from 1024×1024 grid points at small forcings up to 4096×4096 for the highest ones. The two images show the surface plate deflection $\zeta(x,y)$ in the two extreme regimes analyzed here, the lowest forcing amplitude (bottom) and the largest one (up), exhibiting ridgelike deformation.

$f(\cdot)$ is a function of θ only. Its Fourier transform reads $\zeta_{\mathbf{k}} \sim \int rf(\theta)e^{i\mathbf{k}\cdot\mathbf{x}}rdrd\theta \propto \frac{1}{k^3}$, leading to a $1/k^6$ spectrum. Thus in the high forcing regime, the spectrum is dominated by the contribution of the d cones, so that the plate dynamics can be interpreted as oscillating ridges with moving d cones at their edges. Interestingly, it is also different from the Phillips spectrum, that is obtained by balancing the nonlinear with the linear time scales [3], leading to a $1/k^2$ scaling. Assuming $|\zeta_k|^2 \sim k^{-x}$, we obtain $\omega_k^{(1)} \sim k^{4-x}$ so that the condition $\omega_k^{(1)}/\omega_k \sim 1$ gives $x = 2$, leading to the same spectrum than the Rayleigh-Jeans one.

Intermittency. Intermittency for these structures has in fact already been noticed through the computation of the flatness in numerical simulations showing a non Gaussian behavior [30,33]. To analyze further intermittency and anomalous scaling, that is the lack of self-similarity, it is interesting to investigate higher moments using the structure functions [42], $S_p(r) = \langle|\delta\zeta(\mathbf{x},\mathbf{r})|^p\rangle$, where the increment is defined as $\delta\zeta(\mathbf{x},\mathbf{r}) \equiv \zeta(\mathbf{x}+\mathbf{r}) - \zeta(\mathbf{x})$. It is worth emphasizing that statistics of displacement and velocity are the same, since normal variables are a linear combination of both. For plates, the scaling of the energy spectrum is of the form $E_\zeta = k|\zeta|_k^2 \sim k^{-n}$, with $n \geqslant 3$ but a possible logarithmic correction. With this exponent, the cascade is not local and the Wiener-Kintchine theorem does not apply [42], so that

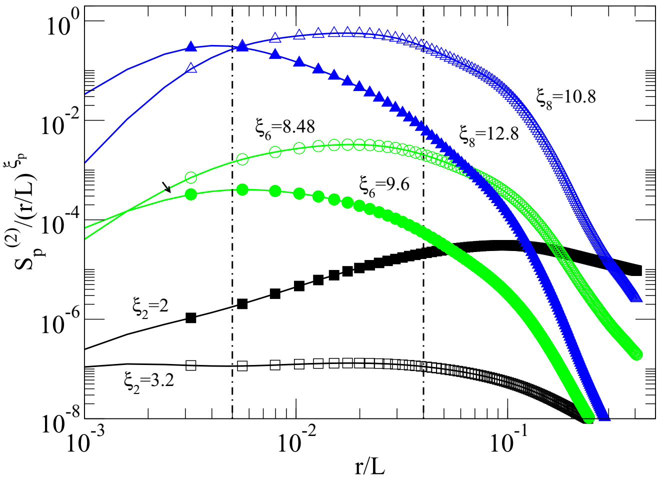

FIG. 2. Compensated structure functions S_p^2 for $p = 2$, 6, and 8 are plotted as functions of r/L, for the strong forcing case ($V7$). They are compensated (divided) by a scaling factor of the form $(r/L)^{\xi_p}$. For $p = 2$, the best fit corresponds to $\xi_p = 3.2$ due to the high forcing, different from $\xi_p = 2$ that would be expected for a the k^{-4} spectrum. For $p = 6$ and $p = 8$ both the Gaussian predictions ($\xi_p = 9.6$ and 12.8 respectively) and the best guessed scalings ($\xi_6 = 8.48$ and $\xi_8 = 10.8$) are presented.

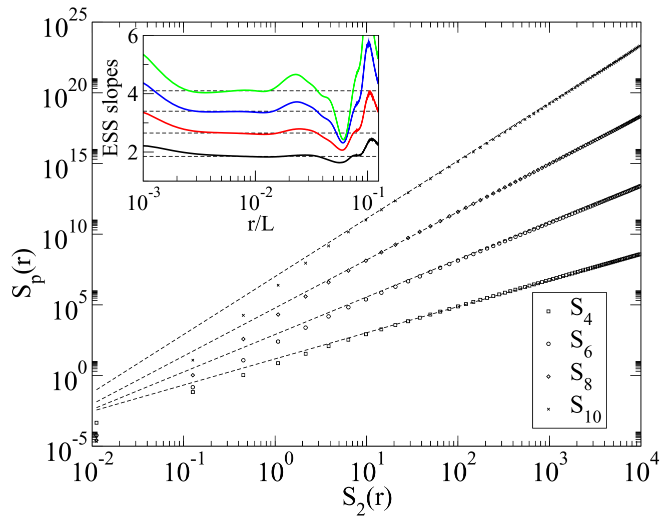

FIG. 3. Plot of the structure function S_p^2 vs S_2^2, for $p = 10$, 8, 6, and 4 from top to bottom. Lines have slopes ξ_p/ξ_2, computed as the logarithmic local slopes shown in the inset as function of r/L. Clear constant slope can be estimated, giving $\xi_p/\xi_2 = 4.05$, 3.4, 2.65, and 1.85 respectively.

the ζ field is expected to be smooth, leading to $S_2(r) \sim r^2$, independent of n. Therefore, second-order difference should be used [27], defined as $\delta\zeta^2(\mathbf{x},r) = \zeta(\mathbf{x}+\mathbf{r}) - 2\zeta(\mathbf{x}) + \zeta(\mathbf{x}-\mathbf{r})$. While in hydrodynamic turbulence, we have the remarkable Kolmogorov four-fifth law for the correlation of third order [42]; no similar relationship exists for the plate equations. However, a semianalytical result can be deduced here from the KZ spectrum: For small forcing the spectrum $|\zeta|_k^2 \sim k^{-4}$ suggests $S_2^2 \sim r^2$ while a steeper exponent is expected at higher forcing, where the spectrum can be seen as a mix of k^{-4} at small scales and k^{-6} at larger ones (corresponding to $S_2^2 \sim r^4$). That leads to the scaling $S_2^2 \sim r^{2\alpha}$, with $1 \leqslant \alpha \leqslant 2$. Then, in the case of Gaussian statistics, one would expect for higher-order structure functions $S_p^2(r) \sim r^p$ for low forcing (neglecting the logarithmic correction) and $S_p^2(r) \sim r^{\alpha p}$ for high forcing. The numerical results for the structure function of order 2 are in line with these findings: For the smallest forcing, we find $S_2^2 \sim r^{\xi_2} = r^{2.2}$, whereas for a stronger one ($V7$ here), $S_2^2 \sim r^{\xi_2} = r^{3.2}$ (see Fig. 2), leading to $\alpha = 1.6$. Figure 2 compares the structure functions of order $p = 6$ and $p = 8$ compensated by the expected self-similar scalings (αp) with those compensated using a best-fit scaling law. We find lower exponent values with the fitted scalings (8.48 instead of $6\alpha = 9.6$ for $p = 6$ and 10.8 instead of $8\alpha = 12.8$ for $p = 8$), demonstrating a discrepancy between Gaussian predictions and actual data for strong forcing, indicating that an intermittent regime is at play. However, the structure functions still exhibit an inertial range over a decade (around $r/L \approx 10^{-2}$).

To investigate further this intermittent property, we extract systematically in all our simulations the exponents ξ_p for the structure functions $S_p^2(r)$ up to $p = 12$. This is done using the extended self-similarity (ESS) technique [43], that consists in computing the logarithmic slope of the curves obtained by plotting $S_p^2(r)$ as a function of $S_2^2(r)$, as shown in Fig. 3. This slope gives in fact directly the ratio ξ_p/ξ_2. While ESS was originally proposed as a form of self-similarity appearing even when inertial range is not detectable [43], we use it here only as a technical tool to extend the range where the scaling can be measured. In particular, we use $S_2^2(r)$ to probe the scaling and to determine a clear inertial range for the. calculations.

Figure 4 presents the ratio of the exponents extracted in this way, ξ_p/ξ_2 as function of p, for the different forcings up to the twelfth order. A Gaussian statistics would correspond to the straight line $\xi_p/\xi_2 = p/2$ drawn in the figure. We observe that for the low forcing $V1$, the results are in agreement with a Gaussian statistics, as expected by the WWT. This is, however, in contradiction with former results obtained experimentally for gravity waves where anomalous scalings were already present at the smallest forcings available [27]. Yet, a clear discrepancy is present for stronger forcing: The variation for the twelfth order is about 20% for $V7$, comparable to what is found for hydrodynamics turbulence (30%). Remarkably, the intermittency saturates for high forcing, at least in the high amplitude limit that we have been able to reach numerically. Such anomalous scaling of the structure functions cannot be reproduced by a linear model, indicating a nontrivial multifractal spectrum of exponents [44,45]. As shown in wave turbulence in the context of magnetohydrodynamics [22], it is useful to build a model which fits the data. Among the various models available [46,47], we have chosen the random-β model [48], with the KZ spectrum considered as a physical constraint. The model describes the cascade in real space looking at scales of size $r_j = 2^{-j}L$, with L being the length at which energy is injected. At the n step of the cascade, the scale r_n splits into scales of size r_{n+1}, but only a fraction $\beta_n (0 < \beta_n \leqslant 1)$ is considered as active. The β_j are independent, identically distributed random

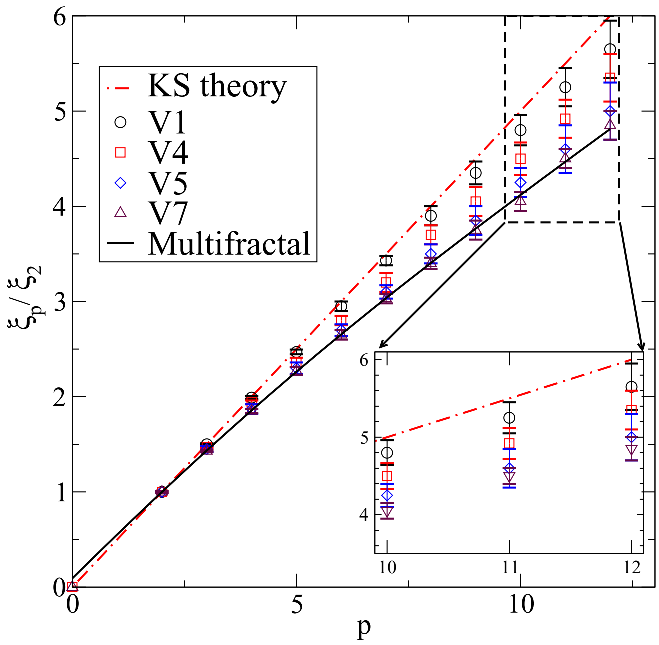

FIG. 4. Structure functions exponent ratio ξ_p/ξ_2 computed using the ESS technique are shown as a function of p for four different forcings. The Gaussian statistics line $\xi_p = \frac{p}{2}$ is shown by the dashed line for comparison. The results can be fitted using the multifractal random β model (solid line), as shown here for the highest forcing $V7$, taking $D_F = 1$ and $x = 0.65$. The inset shows a zoom of the exponent ratio at large p.

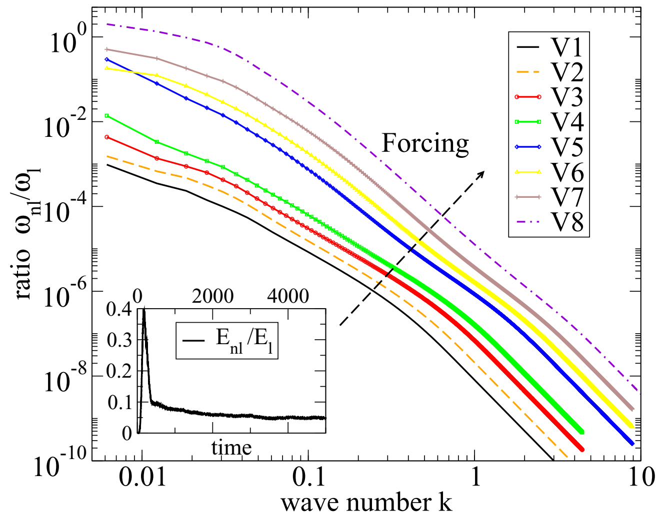

FIG. 5. Nonlinear to linear frequency ratio $\omega_{\mathbf{k}}^{(1)}/\omega_{\mathbf{k}}$ as a function of the wave number for the different forcings. The inset shows the ratio between the nonlinear and the linear energy as a function of time for the highest forcing $V8$.

variables. Therefore, the field fluctuations ζ_n at scale r_n receive contributions only by a fraction $\Pi_{j=1}^n \beta_j$. Taking into account the KZ constraint, one has $\zeta_n \sim \zeta_0 r_n^{3/2} \Pi_{j=1}^n \beta_j^{-1/2}$. All the physics is contained in the distribution of β_j. A simple phenomenological choice is to take $\beta_j = 1$ with probability x and $\beta_j = B = 2^{D_F-2}$ with probability $(1-x)$, where D_F is the dimension of the most singular structures. The corresponding scaling exponents are given in terms of these two parameters $\xi_p = \frac{3}{2} - \log_2[x + (1-x)B^{1-p/2}]$. The case $x = 1$ gives the Kolmogorov-Zakharov scaling. We shall consider x as a free parameter to be estimated by data. Instead, it seems appropriate to consider the ridges between d cones as the most singular and oscillating structures, so that we take $D_F = 1$. The plot of the model deduced shows a very good agreement with numerical results for the highest forcing choosing $x = 0.65$, Fig. 4. From such an agreement, it may be inferred that intermittency is dominated by the oscillations of the ridges. In particular, our results suggest that 35% of the fluctuations are given by these structures.

Discussion. In order to tackle the intermittency origin, some basic hypothesis behind WWT need to be questioned. Since the nonlinear energy terms always remain much lower than the linear ones, varying between 5% and 10% for all the forcings (inset of Fig. 5), no global breakdown of WWT is responsible of the intermittency. But, by analyzing locally in Fourier space the frequency ratio $\omega_{\mathbf{k}}^{(1)}/\omega_{\mathbf{k}}$, Fig. 5 shows that the nonlinear frequencies remain small at large wave numbers for all the forcings, while they become comparable with the linear one at small wave numbers for the highest forcings.

The breakdown of WWT appears thus first at large scales although the spectrum in the inertial ranges still remains within WWT. We can clearly separate our results in two groups: for the four smaller forcings the frequency ratios are everywhere smaller than 10^{-2}, while for the four higher ones, large scales are clearly out of the WWT validity. These two groups are the same as those observed for the spectra in Fig. 1, demonstrating the direct link between the oscillating d-cone spectra, the breakdown of wave turbulence, and the onset of intermittency. Nonetheless, the anomalous scaling was observed for higher statistics at smaller scales, showing that the cascade process triggers a multiplicative amplification of fluctuations.

In conclusion, our numerics show that WWT implies Gaussian statistics at small forcing for vibrating plate turbulence. When the forcing increases, the spectrum changes, exhibiting dynamical ridges and d cones with the breakdown of WWT occurring at large scales. Intermittency appears simultaneously characterized by a multifractal spectrum of exponents which is observed in the inertial range. Observations of intermittency remain an experimental challenge in wave turbulence [26]. In the case of the vibrating plates, the ridgelike structures have been observed mostly numerically, while they were smoothed experimentally by the plate dissipation acting at all scales [33,34]. We hope that this work will motivate experimental estimation of the structure functions of the displacement or the velocity fields, particularly for higher moments than the flatness already studied. More importantly, it would be interesting to characterize experimentally the influence of the oscillating ridges in the dynamics at high forcing and try to relate them to the multifractal model.

Acknowledgment. We want to thank Suzie Protière and Miguel Onorato for fruitful discussions.

[1] V. Zakharov, V. L'Vov, and G. Falkovich, *Kolmogorov Spectra of Turbulence 1: Wave Turbulence* (Springer, Berlin, 1992).
[2] S. Nazarenko, *Wave Turbulence*, Vol. 825 (Springer, Berlin, 2011).
[3] B. Rumpf and A. Newell, Annu. Rev. Fluid Mech. **43**, 59 (2001).
[4] G. J. Komen, L. Cavaleri, M. Donelan, K. Hasselmann, S. Hasselmann, and P. Janssen, *Dynamics and Modelling of Ocean Waves* (Cambridge University Press, Cambridge, UK, 1996).
[5] E. Falcon, C. Laroche, and S. Fauve, Phys. Rev. Lett. **98**, 094503 (2007).
[6] M. Onorato, A. R. Osborne, M. Serio, and S. Bertone, Phys. Rev. Lett. **86**, 5831 (2001).
[7] V. E. Zakharov and N. N. Filonenko, Zh. Prikl. Mekh. I Tekn. Fiz. **5**, 62 (1967) [J. Appl. Mech. Tech. Phys. **8**, 37 (1967)].
[8] A. N. Pushkarev and V. E. Zakharov, Phys. Rev. Lett. **76**, 3320 (1996).
[9] C. Falcon, E. Falcon, U. Bortolozzo, and S. Fauve, Europhys. Lett. **86**, 14002 (2009).
[10] S. Galtier, S. Nazarenko, A. C. Newell, and A. Pouquet, J. Plasma Phys. **63**, 447 (2000).
[11] A. Picozzi, J. Garnier, T. Hansson, P. Suret, S. Randoux, G. Millot, and D. Christodoulides, Phys. Rep. **542**, 1 (2014).
[12] G. Düring, C. Josserand, and S. Rica, Phys. Rev. Lett. **97**, 025503 (2006).
[13] P. Janssen, J. Phys. Oceanogr. **33**, 863 (2003).
[14] A. Majda, D. McLaughlin, and E. Tabak, J. Nonlinear Sci. **7**, 9 (1997).
[15] A. C. Newell, S. Nazarenko, and L. Biven, Phys. D (Amsterdam, Neth.) **152-153**, 520 (2001).
[16] L. Biven, S. Nazarenko, and A. Newell, Phys. Lett. A **280**, 28 (2001).
[17] C. Connaughton, S. Nazarenko, and A. C. Newell, Phys. D (Amsterdam, Neth.) **184**, 86 (2003).
[18] Y. V. Lvov and S. Nazarenko, Phys. Rev. E **69**, 066608 (2004).
[19] Y. Choi, Y. V. Lvov, S. Nazarenko, and B. Pokorni, Phys. Lett. A **339**, 361 (2005).
[20] V. Zakharov, F. Dias, and A. Pushkarev, Phys. Rep. **398**, 1 (2004).
[21] G. L. Eyink and Y.-K. Shi, Phys. D (Amsterdam, Neth.) **241**, 1487 (2012).
[22] R. Meyrand, K. Kiyani, and S. Galtier, J. Fluid Mech. **770**, R1 (2015).
[23] O. Philipps, J. Fluid Mech. **4**, 426 (1958).
[24] E. Kuznetsov, JETP Lett. **80**, 83 (2004).
[25] N. Yokoyama, J. Fluid Mech. **501**, 169 (2004).
[26] F. Haudin, A. Cazaubiel, L. Deike, T. Jamin, E. Falcon, and M. Berhanu, Phys. Rev. E **93**, 043110 (2016).
[27] E. Falcon, S. Roux, and C. Laroche, Europhys. Lett. **90**, 34005 (2010).
[28] S. Nazarenko, S. Lukaschuk, S. McLelland, and P. Denissenko, J. Fluid Mech. **642**, 395 (2010).
[29] É. Falcon, S. Aumaître, C. Falcón, C. Laroche, and S. Fauve, Phys. Rev. Lett. **100**, 064503 (2008).
[30] N. Yokoyama and M. Takaoka, Phys. Rev. E **89**, 012909 (2014).
[31] N. Mordant, Phys. Rev. Lett. **100**, 234505 (2008).
[32] A. Boudaoud, O. Cadot, B. Odille, and C. Touzé, Phys. Rev. Lett. **100**, 234504 (2008).
[33] B. Miquel, A. Alexakis, C. Josserand, and N. Mordant, Phys. Rev. Lett. **111**, 054302 (2013).
[34] T. Humbert, O. Cadot, G. Düring, C. Josserand, S. Rica, and C. Touzé, Europhys. Lett. **102**, 30002 (2013).
[35] L. Landau and E. Lifshitz, *Theory of Elasticity* (Pergamon Press, New York, 1959).
[36] S. Dyachenko, A. Newell, A. Pushkarev, and V. Zakharov, Phys. D (Amsterdam, Neth.) **57**, 96 (1992).
[37] V. M. Malkin, Phys. Rev. Lett. **76**, 4524 (1996).
[38] B. Miquel, A. Alexakis, and N. Mordant, Phys. Rev. E **89**, 062925 (2014).
[39] T. Humbert, C. Josserand, C. Touzé, and O. Cadot, Phys. D (Amsterdam, Neth.) **316**, 34 (2016).
[40] P. Cobelli, P. Petitjeans, A. Maurel, V. Pagneux, and N. Mordant, Phys. Rev. Lett. **103**, 204301 (2009).
[41] B. Miquel and N. Mordant, Phys. Rev. Lett. **107**, 034501 (2011).
[42] A. Monin and A. Yaglom, *Statistical Fluid Mechanics: Mechanics of Turbulence* (Dover, New York, 2007).
[43] R. Benzi, S. Ciliberto, R. Tripiccione, C. Baudet, F. Massaioli, and S. Succi, Phys. Rev. E **48**, R29 (1993).
[44] G. Paladin and A. Vulpiani, Phys. Rep. **156**, 147 (1987).
[45] U. Frisch, *Turbulence: The Legacy of AN Kolmogorov* (Cambridge University Press, Cambridge, UK, 1995).
[46] Z.-S. She and E. Leveque, Phys. Rev. Lett. **72**, 336 (1994).
[47] G. Boffetta, A. Mazzino, and A. Vulpiani, J. Phys. A **41**, 363001 (2008).
[48] R. Benzi, G. Paladin, G. Parisi, and A. Vulpiani, J. Phys. A **17**, 3521 (1984).